Design of HNRD Guide to E-Plane Waveguide Transitions and Directional Couplers by Transverse Resonance Technique

Mitsuyoshi Kishihara*, Isao Ohta**, and Kuniyoshi Yamane*

*Okayama Prefectural University, 111 Kuboki, Soja, Okayama, 719-1197 Japan
**Himeji Institute of Technology, 2167 Shosha, Himeji, Hyogo, 671-2201 Japan

***Abstract* — The present paper designs two types of HNRD guide to rectangular E-plane waveguide transitions with a fractional bandwidth of 10 or more percent for –20dB return loss and a directional coupler of HNRD – E-plane waveguide integrated structure on the basis of the transverse resonance technique(TRT). The theoretical results are in good agreement with results calculated by an em-simulator (Ansoft HFSS).**

I. INTRODUCTION

The NRD guide[1] is an attractive guiding structure at millimeter-wave frequencies because of the low-loss nature, and is applied to an automotive radar[2], a high speed PCM transceiver[3], etc. Generally, the loss of the longitudinally symmetry of the NRD guide causes a mode-coupling between the operative LSM_{01} mode and the parasitic LSE_{01} mode and leads to the degradation of the circuit performance such as increasing of transmission loss and unexpected properties. In order to solve this problem, recently, a new type of NRD guide, Hyper-NRD (HNRD) guide was proposed by Ishikawa et al.[2],[4]. Since the field distribution of the LSM_{01} mode in the (H)NRD guide is analogous to that of TE_{10} mode of a rectangular waveguide, we can utilize in part the (E-plane) rectangular waveguide for construction of an (H)NRD guide system as a launcher and a circuit component. This composite circuit technique enables us more flexibly to design a compact circuit size and desired characteristics.

In this paper, from the above viewpoint, we analyze and design two types of HNRD guide to rectangular waveguide transitions and a directional coupler utilizing HNRD – E-plane waveguide integrated structure by means of the transverse resonance technique(TRT)[5]. As a result, transitions with a fractional bandwidth of 10 or more percent for -20 dB return loss and a directional coupler with a fractional bandwidth of 5 percent are realized. Finally, the validity of the theoretical results is confirmed by comparing with simulation results of an em-simulator (Ansoft HFSS).

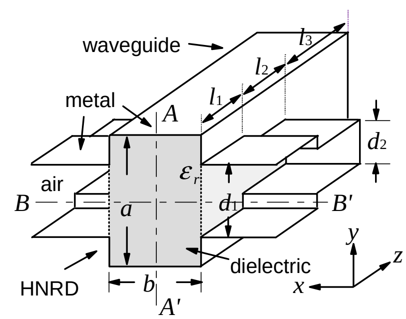

Fig. 1. Structure of an HNRD to waveguide transition.

II. CIRCUIT STRUCTURE AND ANALYTICAL FORMULATION

A. Transition

Figure 1 shows an HNRD guide to rectangular waveguide transition consisting of two HNRD guide regions and a rectangular waveguide, with its geometrical dimensions. The middle HNRD guide works as a quarter-wavelength transformer. The analysis is performed by finding three sets of the resonant lengths, l_1 and l_3, of a cavity constructed of two shorting planes at appropriate distances. Figure 2 illustrates the longitudinal cross section and the equivalent circuit for the structure in Fig. 1. If the scattering matrix of the transition including the discontinuity effect is represented by $\boldsymbol{S}$, we can obtain the following relation:

$$\left\| \boldsymbol{S} - \mathbf{diag}[1/\rho_i] \right\| = 0 \tag{1}$$

where

$$\rho_i = -\exp(-j2\beta_i l_i) \tag{2}$$

is the reflection coefficient seen from the ith port of the transition into the shorted end, and β_i (i=1,3) is the phase constant of the dominant mode of the ith guide. The phase constant for the HNRD guide can be determined by analyzing the uniform HNRD guide.

Because of the symmetrical structure, the analysis requires only a quarter of the entire circuit. In this analysis, since we discuss the transition characteristics between the dominant modes of the HNRD guide and the rectangular

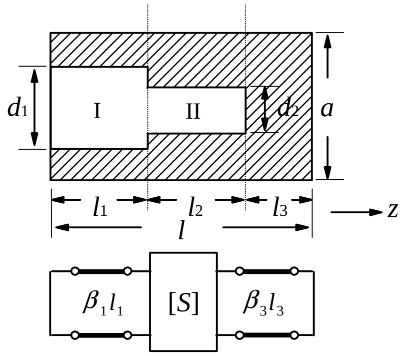

Fig. 2. Longitudinal cross section of the transition and the equivalent circuit.

waveguide, an LSM_{01}-like mode and a TE_{10} mode, the symmetrical planes AA' and BB' are regarded as an electric and a magnetic wall, respectively.

The structure shown in Fig. 1 can be considered as a waveguide discontinuity problem with different cross sections seen along with the *x*-axis. We employ the TRT by expanding the field of each cross section in terms of TE-to-*x* and TM-to-*x* modes and applying the mode-matching method to the discontinuity in the transverse direction.

The field components in the dielectric region can be expanded as follows.

$$\mathbf{E}_t^{(1)} = \sum_{mh} V_{mh}^{(1)} (\boldsymbol{i}_x \times \nabla_t \psi_{mh}^{(1)}) + \sum_{me} V_{me}^{(1)} (-\nabla_t \phi_{me}^{(1)}) \qquad (3)$$

$$\mathbf{H}_t^{(1)} = \sum_{mh} I_{mh}^{(1)} (-\nabla_t \psi_{mh}^{(1)}) + \sum_{me} I_{me}^{(1)} (-\boldsymbol{i}_x \times \nabla_t \phi_{me}^{(1)}) \qquad (4)$$

where

$$\psi_{my,mz}^{(1)} = -P_{my\,mz} \sin\frac{(2m_y+1)\pi\, y}{a} \cos\frac{m_z \pi\, z}{l} \qquad (5)$$

$$\phi_{my,mz}^{(1)} = P_{my\,mz} \cos\frac{(2m_y+1)\pi\, y}{a} \sin\frac{m_z \pi\, z}{l} \qquad (6)$$

ψ_{mh} and ϕ_{me} are the TE and TM scalar potentials under a condition that the plane BB'(*y*=0) is a magnetic wall. The field components in the air region (step region) can also be expanded in a similar way. However, it is necessary to derive the mode functions for the stepped shape.

The potential function for TE mode is expressed by a superposition of the eigen function of the regions I and II. Then, the homogeneous system of equations for the eigenvalue is obtained by considering the continuity conditions at the discontinuity. Finding nontrivial solutions of homogeneous system allows obtaining the eigenvalues k_{cn}, namely, the mode functions. A process for TM mode is analogous.

Figure 3 shows the transverse cross section and its transverse equivalent circuit. The boundary conditions at *x*=*b*/2 are

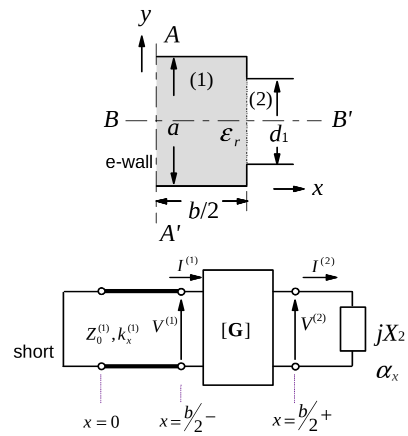

Fig. 3. Transverse cross section and its equivalent circuit.

$$\mathbf{E}_t^{(1)} = \begin{cases} \mathbf{E}_t^{(2)} & \text{on} \quad S_{ap} \\ 0 & \text{on} \quad \text{wall} \end{cases} \qquad (7)$$

$$\mathbf{H}_t^{(1)} = \mathbf{H}_t^{(2)} \qquad \text{on} \quad S_{ap} \qquad (8)$$

where S_{ap} represents the aperture of the stepped shape (regions I and II). Making use of the orthogonality of the potential functions, we obtain the following relations:

$$\boldsymbol{V}^{(1)} = \mathbf{G}\boldsymbol{V}^{(2)} \quad , \quad \boldsymbol{I}^{(2)} = \mathbf{G}^t \boldsymbol{I}^{(1)}, \qquad (9a,b)$$

where

$$\mathbf{G} = \begin{bmatrix} \xi_{nh,mh} & \chi_{ne,mh} \\ \zeta_{nh,me} & \theta_{ne,me} \end{bmatrix}, \qquad (10)$$

$$\xi_{nh,mh} = \int_{Sap} (\boldsymbol{i}_x \times \nabla_t \psi_{nh}^{(2)}) \cdot (\boldsymbol{i}_x \times \nabla_t \psi_{mh}^{(1)}) dS \qquad (11a)$$

$$\chi_{ne,mh} = \int_{Sap} (-\nabla_t \phi_{ne}^{(2)}) \cdot (\boldsymbol{i}_x \times \nabla_t \psi_{mh}^{(1)}) dS \qquad (11b)$$

$$\zeta_{nh,me} = \int_{Sap} (\boldsymbol{i}_x \times \nabla_t \psi_{nh}^{(2)}) \cdot (-\nabla_t \phi_{me}^{(1)}) dS \qquad (11c)$$

$$\theta_{ne,me} = \int_{Sap} (-\nabla_t \phi_{ne}^{(2)}) \cdot (-\nabla_t \phi_{me}^{(1)}) dS \qquad (11d)$$

with abbreviation such as $\boldsymbol{V}^{(1)} = \{\boldsymbol{V}_{mh}^{(1)}, \boldsymbol{V}_{me}^{(1)}\}^t$.

We consider the dielectric and the air regions as a multi-mode transmission lines, and the lines in the air region have infinite lengths, i.e., they are terminated by characteristic impedances (reactances) of each mode. Then, the resonance condition of the transverse equivalent circuit is given as

$$\left\| \mathbf{G}\mathbf{X}_2\mathbf{G}^t + \mathbf{diag}\{ jZ_{0m} \tan(k_{xm} b/2) \} \right\| = 0 \qquad (12)$$

where

$$\mathbf{X}_2 = \mathbf{diag}\{ jX_{2n} \} \qquad (13)$$

$$jX_{2n} = \begin{cases} j\alpha_{xn} / \omega\varepsilon_0 & \text{for TM} \\ \omega\mu_0 / j\alpha_{xn} & \text{for TE} \end{cases}, \qquad (14a)$$

$$Z_{0m} = \begin{cases} k_{xm} / \omega\varepsilon_0\varepsilon_r & \text{for TM} \\ \omega\mu_0 / k_{xm} & \text{for TE} \end{cases}, \qquad (14b)$$

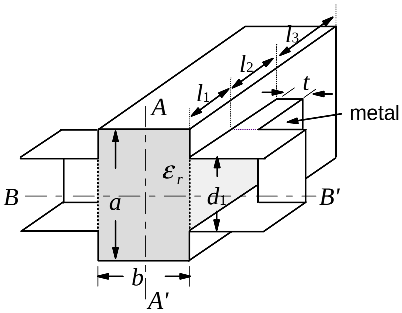

Fig. 4. Another type of the HNRD to waveguide transition.

$$\alpha_{xn} = -\sqrt{-k_0^2 + k_{cn}^2}\ , \tag{15a}$$

$$k_{xm} = \sqrt{\varepsilon_r k_0^2 - \left((2m_y+1)\pi / a\right)^2 - \left(m_z \pi / l\right)^2}\ . \tag{15b}$$

In Equation (12), if one frequency is given, a distance l ($=l_1+l_2+l_3$) is obtained from the condition Det=0.

Figure 4 exhibits another type of the HNRD to waveguide transition. This type of transition has a middle section (λ/4-transformer) with parallel plates shorted at a distance of t. In this case, the transverse equivalent circuit must be modified slightly. The mode functions in each region can be expressed by those of a rectangular waveguide.

B. Directional Coupler

Figure 5 shows a directional coupler composed of HNRD guide – E-plane waveguide cavity. The structure shown in Fig. 5 consists of an E-plane rectangular cavity with four ports, where the HNRD guides are connected through a quarter wavelength transformer section. The cavity region is also filled with dielectric material. It is noticed that the circuit possesses a twofold symmetrical structure for planes AA' and BB'. Therefore, the analysis requires only a quarter part of the circuit as shown in Fig. 6. The symmetry planes AA' and BB' are the four combinations of the electric and/or magnetic wall. The analysis is given by assuming a shorting plane at distance l_1 and finding the respective resonant lengths for four boundary conditions about two symmetry planes.

If the reflection coefficient of each oneport shown in Fig.6 at the input terminal of the transition is represented by $S_{11}^{(i)}$, the reflection coefficient $\rho_1^{(i)}$ seen from the reference plane into the shorted end relates to $S_{11}^{(i)}$ as $S_{11}^{(i)} = 1/\rho_1^{(i)}$ (i=1,2,3,4). Then the scattering matrix for the entire structure can be calculated from the four reflection coefficients $S_{11}^{(i)}$. The remaining procedure of analysis is carried out on the basis of the derived transverse equivalent circuit, analogously. The resonant lengths are determined so as to satisfy the resonance condition of the transverse equivalent circuit.

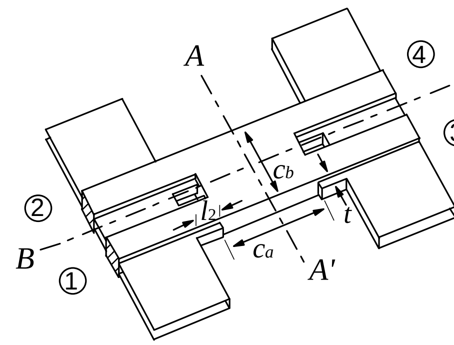

Fig. 5. Structure of a directional coupler composed of HNRD guide and E-plane waveguide cavity.

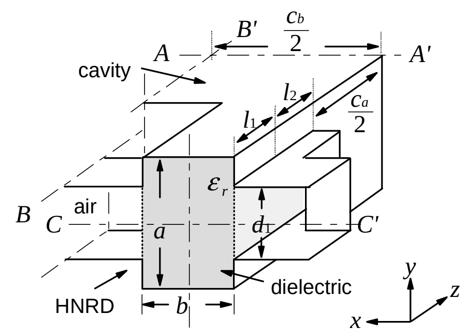

Fig. 6. A quarter part of the directional coupler.

III. Computed Results

We desingned and analyzed two types of transitions and a directional coupler by means of the TRT described in the previous section. The determination of the *S*-parameters of the transitions from (1) requires three different pairs of distances l_1, l_3. A criterion for searching for the resonant lengths is chosen such that the ratio l_1/l_3 has 0.8, 1.0, and 1.25. The distances l_1 and l_3 should be apart from the discontinuities enough to avoid influence of the higher order modes. In this analysis, about a quarter or a half wavelength is chosen as an initial value. Dimensions of a quarter wavelength transformer section are determined by searching for a matching state with varying d_2 and l_2, or t and l_2 at 60GHz.

Figure 7 exhibits three different distances l_1 obtained for a transition of Fig. 1, from which the *S*-parameters shown in Fig. 8 are calculated. Another type of transition in Fig. 4 is similarly designed and a good property is obtained at a center frequency of 60GHz as shown in Fig. 9. The comparison with the results simulated by the HFSS confirms our computed results.

Next, designing of a directional coupler with an integrated structure of the HNRD guide and E-plane waveguide cavity is attempted. The *S*-parameters are calculated by finding the distances l_1 under four different

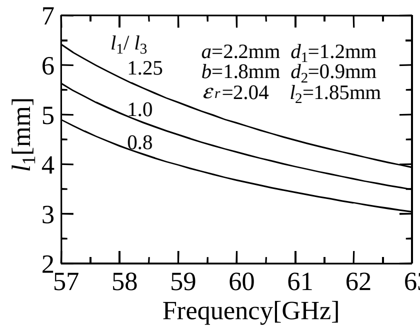

Fig. 7. Three different distances l_1 used for calculation of the *S*-parameters.

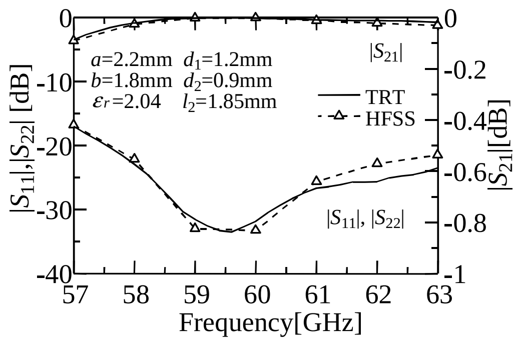

Fig. 8. Frequency characteristics of the *S*-parameters corresponding to Fig. 1.

boundary conditions. The designable parameters for optimization are c_a, c_b, l_2, and t. Figure 10 is the frequency characteristics of the *S*-parameters of the circuit obtained. The center frequency is chosen to 60GHz and the Powell's method is employed for the optimization. In this analysis, it is assumed that no interaction between the HNRD guides has taken place. It is found that this circuit operates sufficiently as a 3dB coupler. The inset in Fig. 10 displays the circuit model used for HFSS's simulation. The HNRD guides are curved for practical use. Although the curved guides are used for the simulation, both results are in good agreement.

IV. Conclusion

We designed two types of HNRD guide to rectangular waveguide transitions and a directional coupler of HNRD – E-plane waveguide integrated structure by the transverse resonance technique. The transitions with a fractional bandwidth of 10 or more percent for –20dB return loss and a directional coupler with a fractional bandwidth of 5 percent were obtained.

Acknowledgements

The authors would like to thank Mr. Sakamoto of Murata Manufacturing Co., Ltd. for his encouragement. In addition, this work was supported by a Grant-in-Aid for Scientific Research (C) (12650389, 2000-2001) from Japan Society for the Promotion of Science.

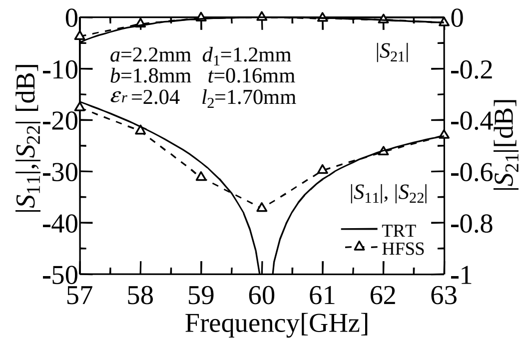

Fig. 9. Frequency characteristics of the *S*-parameters corresponding to Fig. 4.

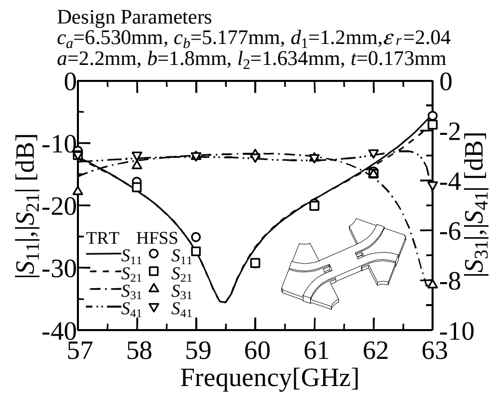

Fig. 10. Frequency characteristics of the *S*-parameters of a directional coupler designed at 60GHz.

References

[1] Y. Yoneyama and S. Nishida, "Nonradiative dielectric waveguide for millimeter-wave integrated circuits," *IEEE Trans. Microwave Theory & Tech.*, vol. 29, no. 11, pp. 1188-1192, Nov. 1981.

[2] Y. Ishikawa, T. Tanizaki, H. Nishida, and Y. Taguchi, "60 GHz band FM-pulse automotive radar front end using new type NRD guide and dielectric lens antanna," *1997 Topical Symposium on Millimeter Waves Proc.*, Hayama (Japan) , pp.155-158, July 1997.

[3] F. Kuroki, K. Ikeda, M. Sugioka, S. Matsukawa, and T. Yoneyama; "High speed PCM transceiver based on the NRD guide technologies at 60GHz band," ibid., pp.119-122, July 1997.

[4] T. Yoneyama, "Millimeter research activities in Japan," ibid., pp.3-6, July 1997.

[5] R. Sorrentino, "Transverse resonance technique," *Numerical Techniques For Microwave And Millimeter-Wave Passive Circuit* (Ed. by T. Itoh, chap. 11), pp.637-696, John Wiley & Sons, Inc., 1989.